

Influence of the Normal Force and Contact Geometry on the Static Force of Friction of an Oscillating Sample

N. Milahin^{1*} and J. Starcevic^{1,2}

¹ Technische Universität Berlin, Berlin, D-10623 Germany

² National Research Tomsk State University, Tomsk, 634050 Russia

* e-mail: natalie.sabelfeld@mailbox.tu-berlin.de

Received February 17, 2014

Abstract—The paper is devoted to an experimental and theoretical investigation of the static friction force between a rapidly oscillating sample and a steel plate. The static frictional force is studied experimentally as function of the oscillating amplitude, the normal force and the contact geometry. A simplest model of tangent contact with a constant friction coefficient is proposed and shows a good agreement with experiment. The static friction force is proved to be a universal function of the ratio of the oscillation amplitude, the indentation depth and to the friction coefficient.

DOI: 10.1134/S1029959914030084

Keywords: tangential contact, contact stiffness, ultrasonic oscillations

1. INTRODUCTION

The influence of ultrasound on the friction force is the subject of research since a solid period of time. The applications range from ultrasonic welding and ultrasonic motors to the atomic force microscopy. If a contact with friction is subjected to oscillations, the static force of friction changes with increasing oscillation amplitude. In the most cases, it decreases [1] up to a level, which may be about an order of magnitude smaller than friction force in the absence of oscillations. This decrease occurs at some characteristic value of l^* . The physical meaning of this characteristic length is not clarified yet. In [2], it was suggested that the characteristic length is an intrinsic parameter of the contacting parameter and does not depend on the geometry of the contact. The amplitude dependence was interpreted in the frame of a stochastic Prandtl–Tomlinsom model [3, 4]. However, in later work [5], it was shown that experimental data can be interpreted from a purely macroscopic point of view, by exact analyzing of a tangential contact with a constant local coefficient of friction. In the present paper, we follow this second path and investigate if it is possible to describe the dependencies on the normal force, the coefficient of friction and the contact geometry in the frame of a tangential contact model without any additional assumptions.

2. THEORETICAL MODEL

If a body is pressed against another and then loaded tangentially, a slip region occurs at the outer border of the contact while the inner parts of the contact remain in the stick state [6, 7]. With growing tangential load, the size of the stick region shrinks and at some load the complete sliding (gross-slip) starts. If the Coulomb law of friction with a constant coefficient of friction μ is assumed to be valid locally, the critical tangential load at which the gross-slip starts is equal to $F_{x,c} = \mu F_n$, where F_n is the normal force. The corresponding relative displacement of the bodies is equal to

$$u_{x,\max} = \mu \frac{E^*}{G^*} d, \quad (1)$$

where E^* and G^* are effective elastic moduli

$$\frac{1}{E^*} = \frac{1-\nu_1^2}{E_1} + \frac{1-\nu_2^2}{E_2}, \quad (2)$$

$$\frac{1}{G^*} = \frac{2-\nu_1}{4G_1} + \frac{2-\nu_2}{4G_2}, \quad (3)$$

E_1 and E_2 are the Young's moduli of contacting bodies, G_1 and G_2 are the shear moduli, ν_1 and ν_2 are the Poisson ratios and d is the indentation depth. The relation $C_M = E^*/G^*$ is the ratio of the normal and tangential stiffness of an axis-symmetrical contact, which we will call the Mindlin ratio [7]. The quantity $u_{x,\max}$ plays a

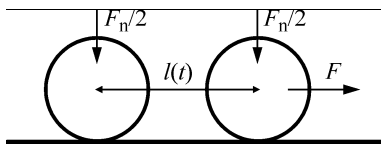


Fig. 1. Schematic presentation of the model: two elastic bodies with curved surfaces are connected with an oscillating bond and are in contact with a planar foundation. The system is being acted upon by a constant external tangential force F . Adapted from [5].

central role both in static and dynamic tangential contacts. This is the only length scale of the problem. If either static or dynamic displacement (oscillation amplitude Δl) is much smaller than $u_{x,max}$ then the oscillation does not play any role at all. If, on the contrary, the oscillation amplitude is much larger than $u_{x,max}$, we have to do with complete sliding. It is physically clear that all characteristics of the contact, including the effective coefficient of friction, can only be functions of the relation $\Delta l/u_{x,max}$. For high frequency oscillations, it is easy to derive analytical relation of the static force of friction as a function of the oscillation amplitude. Let us consider the same model as numerically studied in [5] (Fig. 1) representing two bodies coupled with an oscillating bond, the length of which is changed according to the harmonic law

$$l(t) = l_0 + \Delta l \cos(\omega t). \tag{4}$$

In the absence of the external force F , the oscillation is symmetric and the maximum displacement of each body from the non-stressed reference position is equal to $\Delta l/2$. If this amplitude achieves $u_{x,max}$, the sliding will start at arbitrary small external force F . Thus, the static friction force will vanish if $\Delta l/(2u_{x,max}) = 1$. It is known that the tangential force F_t and the tangential displacement of a single contact of parabolic bodies are related as follows

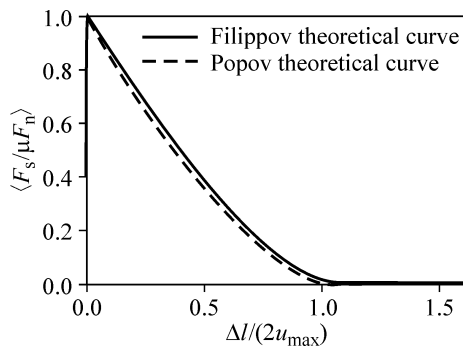


Fig. 2. Dependence of the static force of friction on the oscillation amplitude according to Eq. (6) and numerical simulation carried out in [5].

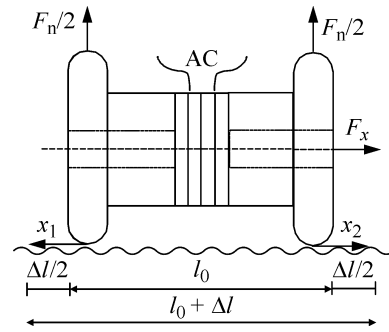


Fig. 3. Schematic of the studied specimen.

$$F_t = \mu F_n \left(1 - \left(1 - \frac{u_x}{\mu C_M d} \right)^{3/2} \right). \tag{5}$$

The difference of this force and the critical force μF_n is the macroscopically observed static force of friction F_s :

$$F_s = \mu F_n \left(1 - \frac{u_x}{\mu C_M d} \right)^{3/2} = \mu F_n \left(1 - \frac{\Delta l}{2u_{x,max}} \right)^{3/2}. \tag{6}$$

This result coincides with the results of numerical simulations [5] (Fig. 2) and will be used in the present paper for fitting of numerical results.

3. EXPERIMENT

A special experiment setup for investigation of tribological systems was built up to measure the friction force. With a special digital ultrasonic generator, the resonance frequency of the specimen is preset at some value, and then the specimen is pressed on the angled plate under a normal force and dragged horizontally with a tangential load. During the moving, the specimen length varies by activation of the piezo-elements which perform mechanical displacements due to the applied voltage (Fig. 3).

The oscillation amplitude of the specimen can be adjusted in the range from 0.015 to 1.500 μm by controlling voltage. The position of the specimen and thus the oscillation amplitude and the oscillation frequency are detected instantaneously with a laser-vibrometer. As

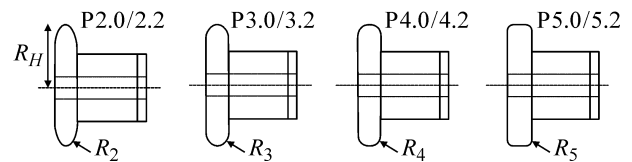


Fig. 4. Schematic of the specimens with different radii, $R_H = 12 \text{ mm}$.

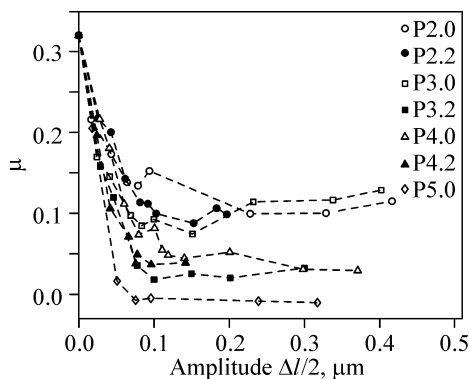
Table 1. Specimen numbers with different radii and weights, specimens with 0.2 are heavy as twice as 0.0

Specimen No.	R , mm	$R_{\text{conv}} = \sqrt{RR_H}$, mm	F_n , N
P2.0	2.5	5.4	0.6
P2.2	2.5	5.4	1.3
P3.0	5.0	7.7	0.7
P3.2	5.0	7.7	1.3
P4.0	10.0	11.0	0.8
P4.2	10.0	11.0	1.4
P5.0	Cylinder $L=5.0$ mm	$\gg 10$	0.7

shown in Fig. 4, four specimens with different radii (Table 1) are investigated. In the individual experiments the specimen is moved with a distance of 100 mm at a constant speed of 0.5 mm/s. The four specimens, numbered with P2.0, P3.0, P4.0 and P5.0, weigh approximately 50 g (the deviation may result from the brazing material and small manufacturing deviations) and oscillate at a frequency of approximately 28 kHz. No extra load is applied, i.e. the specimen weight is equal to the normal force. The specimens P2.2 to P5.2 have the same contact geometry as P2.0 to P5.2, but are double weighted. The relevant amplitude spectrum for these four specimens can be reached at two distinct natural frequencies, approximately 20–25 kHz and approximately 83–90 kHz.

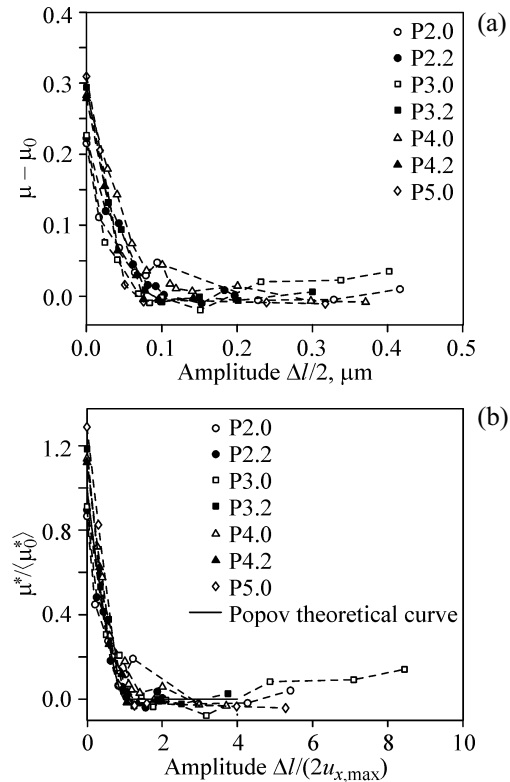
4. RESULTS

The experiments were carried out as follows. First, the coefficient of friction was measured as function of oscillation amplitude $\Delta l/2$. The static friction coefficient μ at $\Delta l = 0$ μm was averaged over all specimens and equated to the value 0.32.

**Fig. 5.** Experimentally obtained coefficient of friction versus a half of the oscillation amplitude.

At amplitude of the order of 0.1 μm , the coefficient of friction decreases to its minimal value and then achieves a plateau or even starts to increase. In other experiments, the effective “friction coefficient” becomes even negative. The reasons for such behavior may be various, including the increased wear at high oscillation amplitude and changes of contact properties or asymmetry of the surface structure. However, the turning point where the frictional force in the most cases changes obviously is clear and significant for determination of the maximum displacement before sliding begins. For each curve, we determined the average value μ_0 of frictional coefficient in the range from 0.1 μm . This value was subtracted from the coefficient of friction, and the quantity $\mu - \mu_0 = \mu^*$ was used for comparison with the above theoretical model (Fig. 6), μ^* at $\Delta l = 0$ μm is defined as μ_0^* .

The resulting curves were fitted to the theoretical dependence by the least squares method, while $u_{x,\text{max}}$ was used as a fitting parameter. According to the theory, all the curves must collapse to one single curve if plotted as function of $\Delta l/(2u_{x,\text{max}})$. Figure 6 shows that this is really the case within the experimental accuracy. The described procedure provides the values of $u_{x,\text{max}}$ for every specimen. The measured values of $u_{x,\text{max}}$ versus

**Fig. 6.** Measured data corrected with the corresponding μ_0 in Fig. 5 (a), fitting according to Eq. (6) (b).

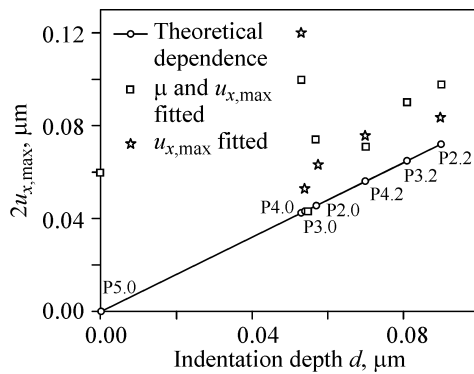


Fig. 7. Displacement $u_{x,\max}$ calculated from measured data according to Eq. (6) versus indentation depth d ; by fitting of both $u_{x,\max}$ and μ^* , and by fitting of $u_{x,\max}$ only.

calculated from the geometry and normal force value of indentation depth d are shown in Fig. 7. The stars represent the measured values and the solid line shows the theoretical relation for $u_{x,\max}$ for the investigated samples with d which was calculated according to the standard equations of contact mechanics [1]. Except for the specimens P4.0 (deviation more than 50%) and P5.0, experimental data have the same trend as theoretical dependency. Discrepancy can be associated with the deflection of the contact shape from the assume one (e.g. because of wear).

In conclusion, our analytical and experimental investigations with specimens of different geometry and with

different normal load support the numerical results of [2].

The author acknowledges valuable discussions and critical comments by V.L. Popov as well as assistance in conduction of experiments by E. Teidelt.

REFERENCES

1. Popov, V.L., *Contact Mechanics and Friction. Physical Principles and Applications*, Springer-Verlag, 2010.
2. Popov, V.L., Starcevic, J., and Filippov, A.E., Simulation of the Influence of Ultrasonic In-plane Oscillations on Static and Sliding Friction and Intrinsic Length Scale of Dry Friction, *Trib. Lett.*, 2010, vol. 39, pp. 25–30.
3. Popov, V.L. and Starcevic, Ya., Tribospectroscopic Study of a Steel-Steel Friction Couple, *Tech. Phys. Lett.*, 2005, vol. 31, no. 4, pp. 309–311.
4. Popov, V.L., Starcevic, J., and Filippov, A.E., Reconstruction of Potential from Dynamic Experiments, *Phys. Rev. E*, 2007, vol. 75, p. 066104.
5. Starcevic, J. and Filippov, A.E., Simulation of the Influence of Ultrasonic In-plane Oscillations on Dry Friction Accounting for Stick and Creep, *Phys. Mesomech.*, 2012, vol. 15, no. 5–6, pp. 330–332.
6. Cattaneo, C., Sul contatto di due corpi elastici: distribuzione locale degli sforzi, *Rendiconti dell'Accademia Nazionale dei Lincei, Series 6*, 1938, vol. 27, pp. 342–348, 434–436, 474–478.
7. Mindlin, R.D., Compliance of Elastic Bodies in Contact, *ASME J. Appl. Mech.*, 1949, vol. 16, pp. 259–268.